Q_A Binding in Reaction Centers of the Photosynthetic Purple Bacterium *Rhodobacter sphaeroides* R26 Investigated with Electron Spin Polarization Spectroscopy†

Johan S. van den Brink,‡ Robertus J. Hulsebosch,‡ Peter Gast,‡ P. J. Hore,§ and Arnold J. Hoff*,‡

Department of Biophysics, Huygens Laboratory, Leiden University, P.O. Box 9504, 2300 RA Leiden, The Netherlands, and Physical Chemistry Laboratory, Oxford University, South Parks Road, Oxford OX1 3QZ, United Kingdom

Received April 18, 1994; Revised Manuscript Received July 28, 1994⊗

ABSTRACT: The relation between quinone (Q_A) binding and electron transport in reaction centers (RCs) of photosynthetic purple bacteria is investigated, using electron spin polarization (ESP) X-band (9 GHz) EPR as a tool to probe for structural changes resulting from charge separation and stabilization and from replacing the native Q_A molecule with other quinones. We present a study of possible changes in Q_A^- binding that might be responsible for the remarkably prolonged lifetime of the charge-separated state at cryogenic temperatures for RCs of *Rhodobacter sphaeroides* R26 cooled under illumination [Kleinfeld, D., et al. (1984) *Biochemistry 23*, 5780−5786]. It is shown that this effect is not caused by a major reorientation of the chromophores. Furthermore, we studied the effects of structurally different quinones functioning as primary electron acceptor in different purple bacteria. With simulations of ESP X-band spectra of the spin-polarized secondary radical pair $P^{\bullet+}Q_A^{\bullet-}$ in menaquinone-reconstituted, Zn^{2+}-substituted RCs of *Rb. sphaeroides* R26, we show that quinone reconstitution is highly selective for site and orientation. Furthermore, we find that a *very small* exchange interaction between $P^{\bullet+}$ and $Q_A^{\bullet-}$ ($|J_{PQ}| \sim 1$ μT) is needed to account accurately for the observed relative line intensities at X-band, without affecting the accuracy of the simulations of reported ESP K-band spectra [Füchsle, G., et al. (1993) *Biochim. Biophys. Acta 1142*, 23−35; Van der Est, A., et al. (1993) *Chem. Phys. Lett. 212*, 561−568]. This pronounced influence of small values for J_{PQ} on the X-band ESP line shape results from cancellation effects of absorptive and emissive contributions to the spectrum, such that small shifts can be observed. The exchange interaction has opposite sign for the native, ubiquinone-containing RC [viz. $J_{P\cdot UQ} = (-0.8 \pm 0.2)$ μT] and the menaquinone-substituted RC [$J_{P\cdot MK} = (+0.3 \pm 0.2)$ μT]. The implications of these observations for electron-transport theory are discussed.

For photoautotrophic growth, electromagnetic energy has to be converted in chemical free energy related to a cross-membrane chemical (proton) potential. In the photosynthetic purple bacteria, this energy conversion takes place in a pigment−protein complex spanning the cytoplasmic membrane, the so-called reaction center (RC).[1] The primary reactions in the RC are (i) light-induced charge separation within ~3 ps from the electronically excited state of the primary donor P, a bacteriochlorophyll (BChl) dimer, producing the primary radical pair $P^{\bullet+}I^{\bullet-}$, where I denotes a bacteriopheophytin (BPhe) molecule, (ii) dark electron transfer within 200 ps from $I^{\bullet-}$ to Q_A, the primary quinone acceptor, creating the secondary radical pair $P^{\bullet+}Q_A^{\bullet-}$, and finally, (iii) within 200 μs the electron reaches Q_B, the secondary quinone acceptor. When electron transfer to Q_B is blocked using chemicals (such as *o*-phenanthrolin), or by removal of Q_B, the secondary radical pair decays by recombination in typically 100 ms at room temperature.

The rate k of nonadiabatic electron transfer processes is given by Fermi's Golden Rule (Marcus, 1956; Jortner, 1976): $k = (2\pi/\hbar)V^2F$, where V is the quantum-mechanical matrix element, which couples the electronic wave functions of the initial and final states, and F is the Frank−Condon factor, which accounts for the total nuclear wave function overlap between donor and acceptor. The matrix elements are expected to depend strongly on the structure of the RC protein and the configuration of the cofactors embedded in the protein [see, e.g., Beratan and Hopfield (1984) and Siddarth and Marcus (1993) and references cited therein]. It is, however, still not possible to calculate accurately electronic couplings from known crystal structures [see, e.g., Plato et al. (1988) and Michel-Beyerle et al. (1988); reviewed by Parson and Warshel (1993)]. Experimentally, the matrix elements can be assessed by measuring the isotropic Heisenberg exchange interaction J between the charged donor and acceptor molecules, because the magnitude of V^2 is proportional to J (Okamura et al., 1979b; Bixon et al., 1989). Methods of determining J include reaction yield detected magnetic resonance (RYDMR) spectroscopy (Norris et al.,

† This research was supported by the Netherlands Foundation for Chemical Research (SON), financed by the Netherlands Organisation for Scientific Research (NWO), and by Twinning Grant No. SC1*-CT90-0569 of the European Commission. P.G. is a research fellow of the Royal Netherlands Academy of Arts and Sciences (KNAW).

* Corresponding author.

‡ Leiden University.

§ Oxford University.

⊗ Abstract published in *Advance ACS Abstracts,* October 15, 1994.

[1] Abbreviations: RC, reaction center; EPR, electron paramagnetic resonance; ESP, electron spin polarization; *Rb.*, *Rhodobacter*; *Rps.*, *Rhodopseudomonas*; *Rc.*, *Rhodocyclus*; PS I, plant photosystem I; BChl, bacteriochlorophyll; BPhe, bacteriopheophytin; P, primary donor; I, intermediairy acceptor; Q_A, primary electron-accepting quinone; Q_B, secondary electron-accepting quinone; UQ, ubiquinone; MK, menaquinone; LDAO, *N,N*-dimethyldodecylamine-*N*-oxide; Brij-58, polyoxyethylene-20-cetyl ether; A, absorption; E, emission.

0006-2960/94/0433-13668$04.50/0

1987; Lersch et al. 1989), measurement of the magnetic field effect (MFE) (Van der Vos, 1994), EPR line shape analysis [see, e.g., Bencini and Gatteschi (1990)], and electron spin polarization (ESP) spectroscopy of the radicals involved in electron transfer [see, e.g., Muus et al. (1977), Hoff (1984), Hore et al. (1987), and Stehlik et al. (1989)].

In all of these methods, the RC contains at least two charges and is subject to considerable Coulombic forces, which could change the structure of the RC compared to that of its neutral state. Such a change would invalidate the direct relation between exchange interaction and the electronic coupling. A notable case is the purported relaxation of the primary photoinduced radical pair $P^{\bullet+}I^{\bullet-}$ (Woodbury & Parson, 1984; Goldstein & Boxer, 1989b). Another example of a possible photoinduced structural change is the photoreduction of Q_A at room temperature, which was suggested to lead to a major structural rearrangement of the cofactors (Kleinfeld et al., 1984). When using the proportionality between J and V^2 for gaining information on the latter parameter, it is clearly important to verify whether such structural changes indeed occur.

The Franck−Condon factor F in the high-temperature limit depends on ΔG_{DA}, the free energy difference between donor and acceptor, and on λ, the nuclear reorganization energy. For lower temperatures, F depends also on specific vibrational modes of the cofactors and/or the medium. [For pertinent analytic expressions, see Jortner (1976) and Marcus and Sutin (1985).] The effect of a change in ΔG_{DA} on the electron transport properties of the RC has been studied in detail for the photoreduction of Q_A (Gunner & Dutton, 1989; McComb et al., 1990; Schelvis et al., 1992). To this end, the native Q_A was replaced by a variety of quinones differing in redox potential, and the quantum efficiency of stable charge separation ($P^{\bullet+}Q_A^{\bullet-}$ formation) measured. In relating the observed changes in quantum efficiency to the change in ΔG_{DA}, it was assumed that other parameters governing electron transport were not affected by the differences in molecular structure between the native Q_A and the substituted quinones. It is again clear that this rather far-reaching assumption needs to be verified.

In this paper, we use electron spin polarization (ESP) spectroscopy to probe possible structural changes related to the formation of the radical pair $P^{\bullet+}Q_A^{\bullet-}$. We first concentrate on the nature of the proposed structural rearrangement of the RC of *Rhodobacter sphaeroides* R26 on freezing under continuous illumination. We also investigate quinone binding in menaquinone-reconstituted RCs of *Rb. sphaeroides* R26. Spectral simulations show that for both cases the quinone is bound in a well-defined position and orientation, corresponding to the geometry of the native ubiquinone. From the $P^{\bullet+}Q_A^{\bullet-}$ ESP spectra, we obtain that J_{PQ} is of opposite sign in ubiquinone- and menaquinone-containing RCs. In the second part of our paper, we discuss two other ESP phenomena observed in RCs, viz. that of ^3P and of $Q_A^{\bullet-}$. We use the EPR signal of $I^{\bullet-}$ in prereduced RCs (Okamura et al., 1979; Tiede et al., 1976; Prince et al., 1977) and the temperature dependence of the ESP of ^3P (Van Wijk et al., 1987, 1988; Van Wijk & Schaafsma, 1988; Proskuryakov et al., 1988; Van den Brink et al., 1994) to show that substituted menaquinone binds to RCs of *Rb. sphaeroides* in much the same way as the native menaquinone to RCs of *Rhodopseudomonas viridis*. The results for the ESP of ^3P and $Q_A^{\bullet-}$ are well explained with a J_{IQ} value for the menaquinone-reconstituted RCs that is more than one order of magnitude larger than that in native RCs.

EXPERIMENTAL PROCEDURES

RCs of *Rb. sphaeroides* R26 were isolated as described by Feher and Okamura (1978). Removal of Q_B and Q_A and reconstitution of Q_A with menaquinone-4 (MK4) were performed according to the method described by Liu et al. (1991a). The yield of the procedures was checked with room-temperature ΔA_{865} measurements to be better than 95% for Q_A,Q_B removal and better than 80% for Q_B removal.

The original detergent LDAO (*N*,*N*-dimethyldodecylamine-*N*-oxide, Fluka) was replaced by 0.1% (w/v) Brij-58 (polyoxyethylene-20-cetyl ether, Sigma), pH 8, using precipitation of the RCs with Bio-Beads SM-2 (Gast et al., 1994). Subsequently, the Fe^{2+} ion was removed (Tiede & Dutton, 1981), and the batch was separated in two parts for the Q_B-depleted sample. Zn^{2+} reconstitution was performed for the MK4-reconstituted sample and for one part of the Q_B-depleted sample by dialyzing against excess 1 mM ZnCl (Debus et al., 1986) in 0.1% (w/v) Brij-58, pH 8. The other part of the Q_B-depleted RCs was used for the EPR measurements of the $P^{\bullet+}Q_A^{\bullet-}$ recombination kinetics on Fe^{2+}-depleted RCs.

The amount of Fe^{2+} removal was checked by monitoring the typical $Fe^{2+}Q_A^{\bullet-}$ $g = 1.8$ EPR signal (Butler et al., 1984) in reduced RCs (Debus et al., 1986). The signal could not be detected in any of the samples used, indicating complete Fe^{2+} depletion. The integrity of the RCs after Fe^{2+} depletion and Zn^{2+} reconstitution was checked with SDS−PAGE. Substantial loss of the H-subunit is observed for the Q_B-depleted RCs after $LiClO_4$ treatment. A small part (~10%) of the H-subunit is still present in the MK4-reconstituted RCs.

A typical EPR sample contained about 60−70% (v/v) glycerol. The final RC concentration was about 50 μM. The samples used for the measurement of the ESP spectrum of the secondary radical pair were, without further additions, either frozen in the dark or frozen rapidly under continuous illumination. For the measurement of the ESP spectra of ^3P and prereduced $Q_A^{\bullet-}$, about 0.3 M sodium ascorbate was added to the samples, after which they were cooled to 80 K under illumination, creating the stable state $PIQ_A^{\bullet-}$.

EPR spectra were obtained using a Varian E-9 spectrometer operating at 9.2 GHz and equipped with a multipurpose TE-101 cavity and an Oxford Helium flow cryostat. The overall instrumental rise time in direct-detection mode was approximately 0.40 μs.

Light-modulated EPR spectra were obtained using an EG&G lock-in amplifier and an ILC 300-W Xe lamp, whose intensity could be modulated with a frequency of up to 1 kHz.

For the time-resolved direct-detection EPR experiments, we used a tunable Ti-Sapphire laser, pumped with a Q-switched Nd-YAG laser (Continuum). The excitation wavelength was 852 nm with 20 mJ/pulse. The duration of the pulse was approximately 20 ns, and the repetition rate was normally 10 Hz, except for the light-frozen samples, where we used 2 Hz. The direct-detection EPR signal was recorded using a boxcar integrator (Stanford Research Systems, Inc.).

Kinetic traces were averaged using a LeCroy 9410 150-MHz digital oscilloscope, equipped with a signal-averaging

facility. Data processing was done on a personal computer. ESP spectra of $P^{\bullet+}Q_A^{\bullet-}$ were simulated using the spin-correlated radical pair model of electron spin polarization (Hore et al., 1987; Stehlik et al., 1989). The possibility of producing polarization in the primary radical pair $P^{\bullet+}I^{\bullet-}$ in the MK4-reconstituted, Zn^{2+}-substituted RCs was ignored because of its short measured lifetime at 10 K (~150 ps, H. J. M. Schelvis and J. S. van den Brink, unpublished results). Unresolved hyperfine splittings and the natural line width were incorporated in the Gaussian line widths ΔB_P and ΔB_Q. The simulations were performed on a SUN Sparc 2 and a Silicon Graphics Personal Iris workstation.

RESULTS AND DISCUSSION

Light-Induced Changes on Reduction of Q_A. When RCs, in which the prereduced $Q_A^{\bullet-}$ is magnetically decoupled from the non-heme Fe^{2+} ion by its removal and/or substitution with diamagnetic Zn^{2+}, are illuminated at cryogenic temperatures, the (normally absorptive) dark EPR signal of $Q_A^{\bullet-}$ becomes emissively polarized (Gast & Hoff, 1979; Gast et al., 1982, 1983). Hore et al. (1993) used simulations of the Q-band (35 GHz) ESP spectrum of $Q_A^{\bullet-}$ at 80 K for determining the sign and magnitude of the exchange interaction between $P^{\bullet+}$ and $I^{\bullet-}$, J_{PI}, thus constraining ΔG_{PI} to be in the range $-600\ cm^{-1} \leq \Delta G_{PI} \leq -200\ cm^{-1}$ (Bixon et al., 1991). This result was interpreted to indicate that the sequential and superexchange mechanisms for initial charge separation operate in parallel at all temperatures [for a discussion of the various mechanisms of charge separation, see Bixon et al. (1991) and references cited therein]. The results of Hore et al. (1993) critically depend on knowledge of the RC structure obtained by X-ray crystallography. Whether they are valid for physiological conditions, however, is uncertain, since Q_A is reportedly subject to a structural rearrangement on reduction at room temperature (Kleinfeld et al., 1984). Thus, the prereduced quinone may have a different orientation compared to the dark-adapted, neutral RC.

A light-induced structural change of the RC was put forward by Kleinfeld et al. (1984) to explain the observed difference in the rate of forward electron transport from Q_A to Q_B, and in the recombination kinetics of $P^{\bullet+}Q_A^{\bullet-}$, at cryogenic temperatures after freezing the RCs in the dark or under continuous illumination (i.e., in the charge-separated state). The recombination is slowed down considerably and shows a nonexponential behavior in light-frozen RCs (Kleinfeld et al., 1984). This phenomenon could be explained by assuming a heterogeneity in $P-Q_A$ distances, with the quinone moving about 0.2−0.3 nm *away* from P on charge separation. Recently, time-resolved voltage measurements at room temperature indicated that, within 200 μs after the generation of $P^{\bullet+}Q_A^{\bullet-}$, a charge is displaced in a direction perpendicular to the membrane. This process, which apparently is the rate-limiting step for the Q_A to Q_B electron transfer, could involve a 0.2-nm shift of Q_A *toward* P and/or protonation of $Q_A^{\bullet-}$ (Brzezinski et al., 1992). Assuming that there are no drastic changes of the protein lattice associated with electron transfer from $Q_A^{\bullet-}$ to Q_B, the Q_A binding pocket in *Rb. sphaeroides* R26 only allows for a displacement of the quinone in a direction *parallel* with the membrane (Allen et al., 1988). This shift has no electrogenic effect and does not result in a *larger* $P-Q_A$ distance.

The origin of the light-induced changes on generation of the secondary radical pair is as yet unclear and apparently cannot be accounted for by any lateral displacement of the Q_A molecule. Other mechanisms may be relevant, such as a nuclear relaxation process or a local change of the redox properties of the protein lattice, affecting the Frank−Condon factor such that the recombination of $P^{\bullet+}Q_A^{\bullet-}$ is slowed down and electron transfer to Q_B is facilitated.

We have employed ESP spectroscopy to investigate further the nature of the light-induced changes, since the ESP spectrum of the secondary radical pair $P^{\bullet+}Q_A^{\bullet-}$ critically depends on the relative orientations of the radicals and their mutual interactions (Hoff, 1984; Hore et al., 1987; Stehlik et al. 1989), which, as mentioned above, may influence both V^2 and F.

Light-Induced Changes of the $P^{\bullet+}Q_A^{\bullet-}$ Recombination Kinetics. The kinetic experiments of Kleinfeld et al. (1984) were carried out using Fe^{2+}-containing, Q_B-depleted RCs solubilized in the detergent LDAO. The spin-polarized signal from $P^{\bullet+}Q_A^{\bullet-}$, however, can only be observed and described accurately in RCs in which the Fe^{2+} ion is substituted with diamagnetic Zn^{2+}. Since this Zn^{2+} substitution procedure is not possible for LDAO-RCs, the LDAO was exchanged for the detergent Brij-58.

We first repeated the experiment of Kleinfeld et al. (1984) for the native, Q_B-depleted RCs solubilized in Brij-58, detecting the recombination from the secondary radical pair using the 100-kHz magnetic field-modulated X-band EPR signal. For the dark-frozen sample, we found a single-exponential decay with $\tau = 30.0$ ms (see Figure 1A), comparable with the literature value for LDAO-RCs (Kleinfeld et al., 1984). The light-frozen sample clearly did not decay with a single exponential (Figure 1A). This decay was characterized by a biexponential function, with $\tau_1 = 41.8$ ms (55%) and $\tau_2 = 153$ ms.

For the Fe^{2+}-depleted sample, we found a biexponential decay for the dark-frozen RCs, with $\tau_1 = 8.3$ ms (59%) and $\tau_2 = 48.5$ ms (Figure 1B). This result, which is comparable with that reported by Parot et al. (1987) for native (Fe^{2+}-containing) RCs, suggests that in Fe^{2+}-depleted RCs two distinct conformational states pre-exist in the dark. Since we did not find any indication for such pre-existing conformational states in the native, Fe^{2+}-containing RC, it is likely that in the RCs used by Parot et al. (1987) the Fe^{2+} was, at least partially, removed. Upon freezing the Fe^{2+}-depleted RCs under illumination, the decay again was slowed down (see Figure 1B), with characteristic decay times $\tau_1 = 13.2$ ms (57%) and $\tau_2 = 142$ ms. This indicates that RCs preexisting in a fast-decaying state do not exhibit a light-induced change (τ_1 is little affected), in contrast to the slowly-decaying RCs. This phenomenon could well be related to two distinct positions of Q_A in Fe^{2+}-depleted RCs lacking the H-subunit (Liu et al., 1991b). Only the native position of Q_A would then show a light-induced change. Our results for light-frozen Fe^{2+}-depleted RCs again compares well with the results of Parot et al. (1987) for light-frozen native RCs, who found that the slowly decaying component τ_2 changes from 37 to 105 ms when the sample is frozen under illumination, in contrast to τ_1 which did not depend on freezing conditions.

Reconstitution with a Zn^{2+} ion results in a single-exponential decay for dark-frozen RCs, comparable with that for the native RCs [cf. the room temperature results shown by Debus et al. (1986)], with a decay time of $\tau = 36.5$ ms (see Figure 1C). This result indicates that RCs containing a divalent metal ion exist in one predominant conformation,

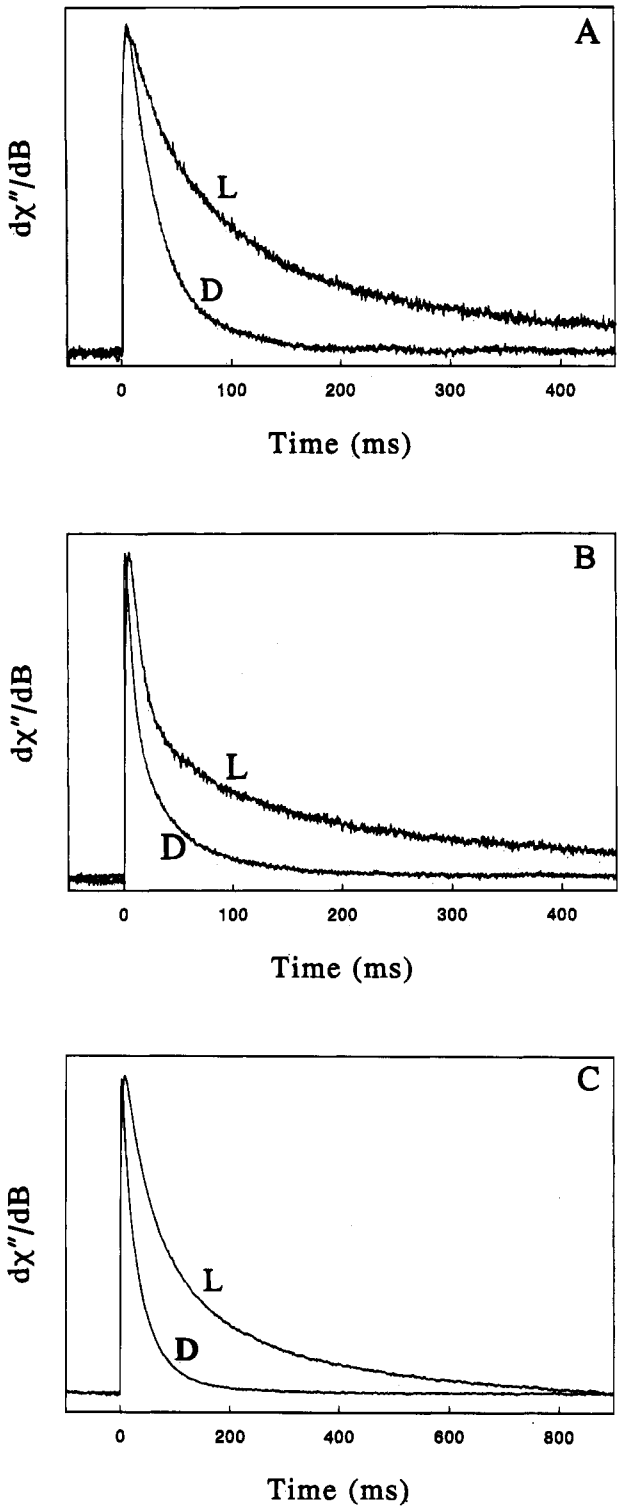

FIGURE 1: $P^{\bullet+}Q_A^{\bullet-}$ recombination kinetics at 4 K obtained from the 100-kHz magnetic-field modulated X-band EPR signals for (A) Q_B-depleted, Fe^{2+}-containing, (B) Q_B-depleted, Fe^{2+}-depleted, and (C) Q_B-depleted, Zn^{2+}-substituted RCs of *Rb. sphaeroides* R26 solubilized in Brij-58 (pH 8). Traces A and B are averages of 400 transients induced by an actinic flash of a Xe flashlamp. Trace C is the average of 900 transients induced by laser excitation at 850 nm. D and L denote dark- and light-frozen, respectively. Recombination times from (bi-)exponential fits are given in the text.

which is distorted when the metal ion has been removed. For RCs frozen under continuous illumination this changes to a biexponential decay with $\tau_1 = 57.2$ ms (55%) and $\tau_2 = 245$ ms. The kinetic experiments thus unambiguously prove that Zn^{2+}-substituted RCs of *Rb. sphaeroides* R26 exhibit a light-induced change comparable with that observed for

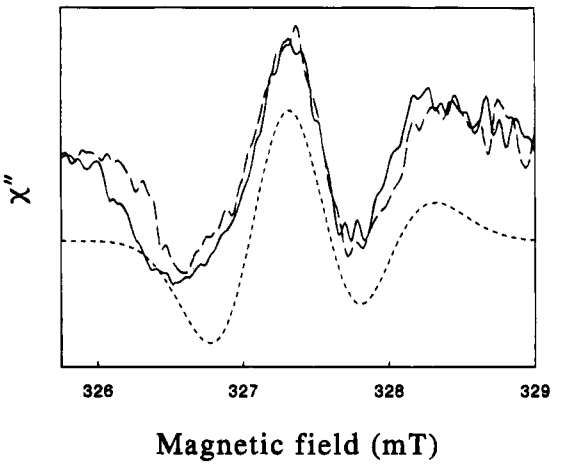

FIGURE 2: Direct-detection EPR spectra of the secondary radical pair ($P^{\bullet+}Q_A^{\bullet-}$) in Q_B-depleted, Zn^{2+}-reconstituted RCs of *Rb. sphaeroides* R26 frozen in the dark (solid line) and under continuous illumination (dashed line). The lower dashed line represents a simulated line shape, using parameters discussed in the text. The corresponding $P^{\bullet+}Q_A^{\bullet-}$ recombination kinetics are shown in Figure 1C. Spectra were obtained using laser excitation and a boxcar integrator (see Experimental Procedures). The time window of the boxcar was 0.5−2.5 μs, and it was used in DC mode. $T = 20$ K; microwave frequency, 9.153 GHz; microwave power, 1 mW; scan time, 2 h; time constant, 15 s. The repetition rate of the laser was 2 Hz.

native, Fe^{2+}-containing RCs. Depletion of the H-subunit apparently does not affect the capability of the RC to show a light-induced change of the $P^{\bullet+}Q_A^{\bullet-}$ recombination rate. This would imply that Q_A is bound in the native position and orientation in RCs lacking the H-subunit, but containing a divalent metal ion. This has also been proposed by Liu et al. (Liu et al., 1991b; Schelvis et al., 1992), who showed that the electron transfer rate from $I^{\bullet-}$ to Q_A is not affected in this case, whereas it changes in RCs containing all three subunits, but lacking the divalent metal ion. Below we show that Q_A-binding is indeed *not* sensitive to depletion of the H-subunit in Zn^{2+}-substituted RCs, viz. the quinone retains its native position and orientation.

Light-Induced Changes and the Polarization Pattern of $P^{\bullet+}Q_A^{\bullet-}$. Furnished with the above information concerning the kinetic changes observed for Zn^{2+}-substituted RCs frozen in the charge-separated state, we can now attempt to investigate the possible occurrence of structural changes of the Q_A binding-pocket in this system, using ESP spectroscopy. Preparing two identical samples, one of which is frozen in the dark and the other under continuous illumination, allows the determination of structural changes associated with the formation of $P^{\bullet+}Q_A^{\bullet-}$. Figure 2 shows the direct-detection X-band ESP spectra of the radical pair $P^{\bullet+}Q_A^{\bullet-}$ for light- and dark-frozen, Q_B-depleted RCs. Since the secondary radical pair in the light-frozen RC is long-lived, both spectra were obtained with a repetition rate of the laser of 2 Hz. A boxcar averager was used for the detection of the light-induced direct-detection EPR signal. In Figure 2, the spectra have been normalized to show that their shapes are virtually identical. Because the samples were identical, with tubes from the same quartz stock, absolute signal amplitudes also could be compared. The signal of the light-frozen RCs was about 3 times less intense than that of the dark-frozen RCs. This significant decrease of the ESP signal amplitude cannot be accounted for solely by the interference of the repetion rate of the exciting laser flash with the slower decay of the light-frozen sample. This could result at most

in a reduction of 15% in signal amplitude, as follows from the kinetic traces of Figure 1C. We discuss below that the decrease in amplitude may be caused by a higher degree of cancellation of the (enhanced absorptive and emissive) components that compose the experimental spectrum (Stehlik et al., 1989; Hore, 1990).

The spectra of Figure 2 deviate slightly from the spectrum obtained by Füchsle et al. (1993). We found the same, well-reproducible pattern for (dark-frozen) RCs from different preparations (Q_B-containing *and* Q_B-depleted). We will show below that small differences in the exchange interaction J_{PQ} between $P^{\bullet+}$ and $Q_A^{\bullet-}$, related to slight differences between samples, may account for the observed differences at X-band. These differences between samples are well-known from the observation of slightly different $P^{\bullet+}Q_A^{\bullet-}$ recombination rates for RCs from different preparations (Kleinfeld et al., 1984; Parot et al., 1987), which could be related to a difference in preparation method (RCs containing or lacking the H-subunit) or to biological variability (e.g., the bacteria used were from a different strain or were grown under different conditions).

The virtual identity of the ESP spectra of dark- and light-frozen samples enabled us to delimit the structural changes that purportedly cause the difference in recombination kinetics of the two preparations. To this end, the ESP spectra were simulated with extensive variation of the structural parameters. For the simulation of the ESP signal of the secondary radical pair, a large number of parameters are required, such as the g tensors of $P^{\bullet+}$ and $Q_A^{\bullet-}$ and their orientations, the line widths of $P^{\bullet+}$ and $Q_A^{\bullet-}$, the magnitude and orientation of the (axial) dipolar interaction between $P^{\bullet+}$ and $Q_A^{\bullet-}$, D_{PQ}, and the magnitude of J_{PQ}. Several recently published studies allow us to fix values for most of these parameters and to obtain a narrow parameter space for which the spectra can be simulated.

As a starting point, we used the parameters found by Stehlik and co-workers (Füchsle et al. 1993; Van der Est et al., 1993) from a simulation of their K-band (24 GHz) ESP spectra of Zn^{2+}-substituted RCs frozen in the dark. They used the g tensor components of $P^{\bullet+}$ in *Rb. sphaeroides* and the orientation of the principal axes of g_P in the crystallographic frame of reference from a recent W-band (95 GHz) single-crystal study (Klette et al., 1993). In this study, four possible orientations of the g tensor of P^+ were obtained, whereas simulations of the K-band ESP spectra showed that orientation I for g_P (Klette et al., 1993) is to be preferred (Füchsle et al., 1993; Van der Est et al., 1993). The g tensor for $Q_A^{\bullet-}$ was obtained at W-band by Burghaus et al. (1993). The orientation of the g tensor of $Q_A^{\bullet-}$ and the direction of the $P^{\bullet+}Q_A^{\bullet-}$ dipolar axis with respect to the crystallographic frame were calculated for the ubiquinone in the native RC, using the crystal structure P4RCR (Komiya et al., 1988). The magnitude of the dipolar interaction between $P^{\bullet+}$ and $Q_A^{\bullet-}$, D_{PQ}, was calculated from the PQ distance obtained from the crystal structure, viz. $D_{PQ} = -0.12$ mT.

The above set of parameters, however, did not reproduce the X-band ESP spectrum well, either that reported by Füchsle et al. (1993) and Van der Est et al. (1993) or the spectra of Figure 2. Since we wish to use X-band ESP spectroscopy to probe the RC structure, this is a very unsatisfactory situation, which was also noted by Füchsle et al. (1993) and Van der Est et al. (1993). They concluded that the poor simulation at X-band could not be remedied by variation of the parameter set based on the K-band ESP spectra. Note that the latter spectra are more sensitive to small changes in the g tensors of $P^{\bullet+}$ and $Q_A^{\bullet-}$ than the X-band spectra, which are more sensitive to small variations of the magnetic couplings.[2]

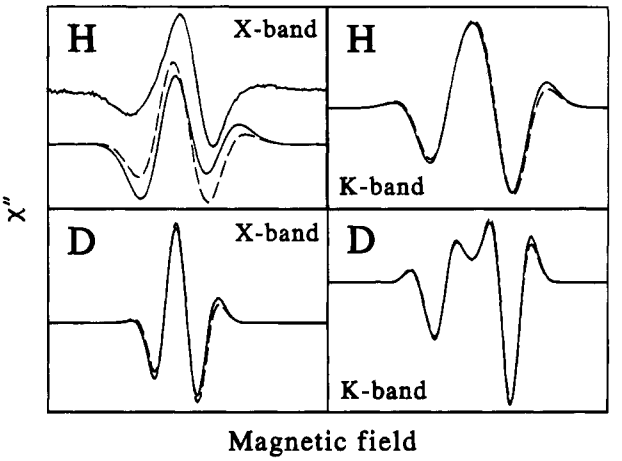

FIGURE 3: Simulations of the ESP X- and K-band spectra of the secondary radical pair ($P^{\bullet+}Q_A^{\bullet-}$) in protonated (H) and perdeuterated (D) UQ-containing, Zn^{2+}-substituted RCs of *Rb. sphaeroides* R26. All parameters used for the simulations are discussed in the text. The solid line is identical with the simulations by Füchsle et al. (1993) and Van der Est et al. (1993); the dashed line represents our improved simulation including $J_{PQ} = (-0.9 \pm 0.2)$ μT, which is virtually identical with all *experimental* spectra shown by Füchsle et al. (1993) and Van der Est et al. (1993), shown as the upper solid line for protonated RCs at X-band [reprinted with permission from Füchsle et al. (1993)]. It can be seen that $J_{PQ} \neq 0$ affects the protonated X-band spectrum most pronouncedly, since in that case the highest degree of cancellation occurs (see text). *All* spectra are simulated well now using *one* parameter set, which can be used as a starting point for further research on modified RCs.

We found that a small additional isotropic magnetic interaction J between $P^{\bullet+}$ and $Q_A^{\bullet-}$ profoundly influences the X-band spectra without affecting the K-band spectra. Keeping the parameter set of Stehlik et al. (Füchsle et al. 1993; Van der Est et al., 1993), but adding $J_{PQ} = (-0.9 \pm 0.2)$ μT, we accurately simulated *both* the K-band *and* the X-band spectra of Stehlik et al. (Füchsle et al. 1993; Van der Est et al., 1993). As shown in Figure 3, only the X-band ESP spectrum for protonated RCs is very sensitive for J_{PQ}. The spectra of Figure 2 also could be simulated well with the same parameter set, *except* $J_{PQ} = (-0.3 \pm 0.2)$ μT (lower dashed line in Figure 2). This provides us with a complete parameter set, which we have used further in studying structural modifications. As mentioned above, the small difference in J_{PQ} is probably related to small variations in the sample preparation procedures or to biological variability. The *structure* of our RCs, lacking the H-subunit, and those of Stehlik et al. (Füchsle et al. 1993; Van der Est et al., 1993) is identical, however, with the X-ray crystallographic structure to within the experimental error.

The, at first sight surprisingly large, effect of small values of J_{PQ} on the X-band ESP spectrum is explained by the large degree of cancellation of the (enhanced absorptive or emissive) components contributing to the ESP spectrum of a correlated radical pair (Hore et al., 1987; Hore, 1990; Stehlik et al., 1989). Small shifts induced by varying one

[2] At higher frequency (and field), the spin hamiltonian is dominated by g anisotropy. The K-band spectrum is therefore much less sensitive to magnetic field-independent terms such as those containing the magnetic couplings.

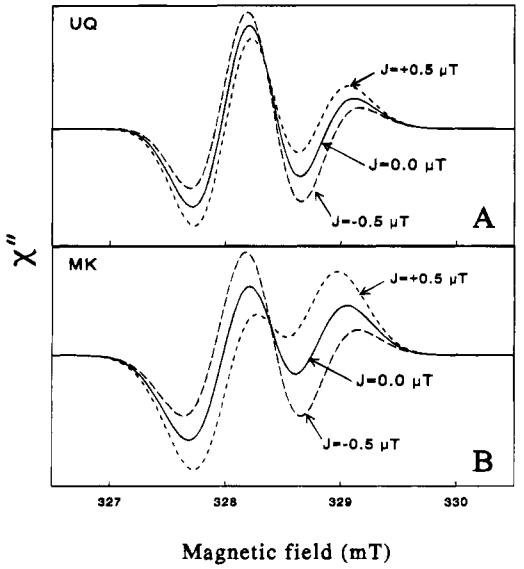

FIGURE 4: Simulations showing the effect of J_{PQ} on the ESP X-band spectrum of the radical pair ($P^{\bullet+}Q_A^{\bullet-}$) in (panel A) UQ10-containing and (panel B) MK4-reconstituted, Zn^{2+}-substituted RCs of *Rb. sphaeroides* R26.

parameter, e.g., J_{PQ}, then result in large differences in the sum spectrum (see also Figure 4).

The X-band ESP spectrum for light-frozen RCs closely resembles that for dark-frozen RCs (Figure 2) except for a 60−70% decrease in intensity. This may imply a higher degree of cancellation of the spectral components. We varied the orientation of the semiquinone radical with a constant value for D_{PQ}, and J_{PQ} within the range of −1.0 to 1.0 μT. Because the spectra of Figure 2 have a virtually identical line shape, but a decreased intensity for the light-frozen sample, the range of angles compatible with a satisfactory simulation of the X-band ESP spectra is narrow: allowed (counterclockwise) rotations are (i) a rotation of −3° to +2° around the g_x axis of the quinone [i.e., the axis connecting the carbonyl oxygens (Hales, 1975; Burghaus et al., 1993; Füchsle et al., 1993)] and (ii) a rotation up to +7° around its g_z axis (i.e., the axis perpendicular to the aromatic ring). For these reorientations of Q_A, the spectral *shape* does not change, although the *amplitude* does vary (it decreases by a factor of about 3 while rotating only 2° from the dark-adapted orientation). In all other cases, the line shape of the ESP spectrum changes profoundly. These changes are related to the extent to which the above-mentioned cancellation of the spectral components occurs. Since the ESP spectra for dark-frozen and light-frozen RCs are virtually identical, structural changes accompanying freezing under continuous illumination are limited to the above-mentioned allowed rotations, which do not affect the spectral shape.

Considering the narrow allowable parameter space, we propose that the observed differences in electron-transfer rates are mainly related to Coulombic relaxation effects of the *protein* upon producing two charged radicals in the protein matrix at room temperature. These effects may include nuclear relaxations and differences in the *local* free energy of the protein and/or Q_A. The latter effect may be caused by minor distortions only of the orientation of the methoxy groups of UQ10, related to slight changes of the protein backbone near the Q_A-binding pocket altering the steric hindrance of the methoxy groups. Conformation-dependent π-donation of the methoxy substituents, as well

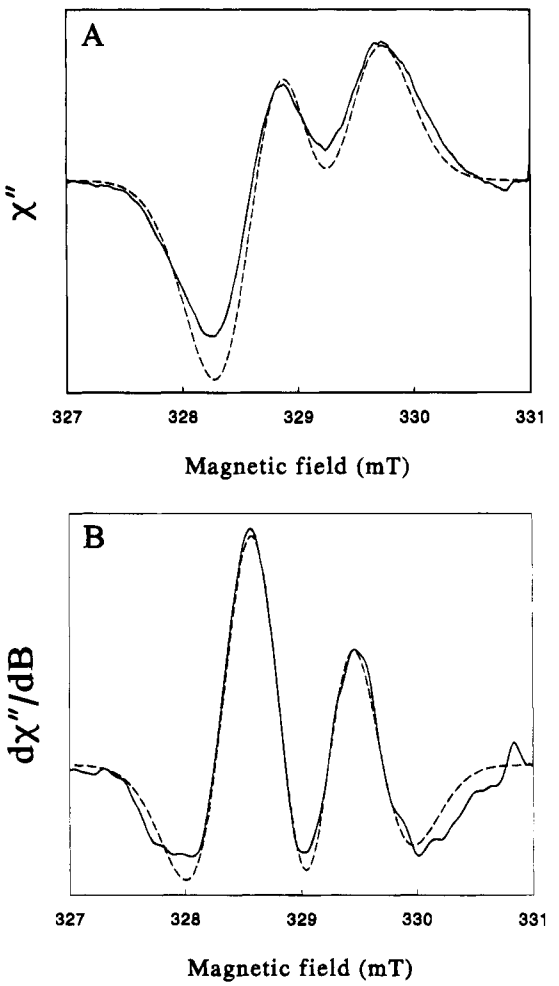

FIGURE 5: (A) Direct-detection EPR spectrum of the secondary radical pair ($P^{\bullet+}Q_A^{\bullet-}$) in RCs of *Rb. sphaeroides* R26, reconstituted with MK4 (solid line). The spectrum was obtained using laser excitation (see Experimental Procedures) and a boxcar integrator. The time window of the boxcar was 0.5−2.5 μs, and it was used in DC mode. T = 10 K; microwave frequency, 9.21 GHz; microwave power, 5 mW; scan time, 30 min.; time constant, 10 s. The dashed line is a simulation using the parameters discussed in the text. For the line widths we used ΔB_P = 0.65 mT and ΔB_{MK4} = 0.69 mT. (B) Numerically obtained first-derivative spectrum (solid line) and corresponding simulation (dashed line). These spectra are given for comparison with polarized $P^{\bullet+}Q_A^{\bullet-}$ EPR spectra published elsewhere [see Snyder and Thurnauer (1993) and references cited therein].

as different (inter- and/or intramolecular) Coulombic or dipolar interactions of the carbonyl oxygen with nearby charges has been shown to change the quinone's electron affinity profoundly (Robinson & Kahn, 1990). A statistical distribution of structural changes resulting from the protein relaxation could easily result in an apparent biphasic recombination rate.

Quinone Reconstitution. Spin Polarization of the $P^{\bullet+}Q_A^{\bullet-}$ Radical Pair. The direct-detection ESP spectrum of the secondary radical pair, $P^{\bullet+}Q_A^{\bullet-}$, for MK4-reconstituted, Zn^{2+}-substituted RCs is shown in Figure 5A. For comparison with previous work on bacterial RCs and PS I (Snyder et al., 1991; Snyder & Thurnauer, 1993), Figure 5B shows the first-derivative spectrum, obtained by numerical differentiation. Dashed lines represent the optimized spectral simulation, calculated using the correlated radical pair model (Hore et al., 1987; Stehlik et al., 1989). Polarization produced in the primary radical pair can be neglected (Snyder & Thurnauer, 1993), since its lifetime is about 150 ps in the Zn^{2+}-

Table 1: Principal Values of the g Tensors of P_{865} (Burghaus et al., 1993), P_{700} (Prisner et al., 1993), UQ, and MK (Burghaus et al., 1993)

	P_{865}	P_{700}	UQ	MK
g_x	2.0033	2.0030	2.0066	2.0056
g_y	2.0024	2.0026	2.0054	2.0049
g_z	2.0021	2.0023	2.0022	2.0022

substituted RCs (H. J. M. Schelvis and J. S. van den Brink, unpublished results).

For the simulations of the ESP spectrum of $P^{\bullet+}MK4^{\bullet-}$, we use the g_P tensor mentioned above and for MK4 the g values for another 1,4-naphthoquinone derivative, viz. phylloquinone or vitamin K1 (Burghaus et al., 1993), the first metastable electron acceptor in PS I [see, e.g., Snyder (1991) and references cited therein; see Table 1]. The latter g values agreed with the (lower resolution) Q-band EPR spectrum of $MK4^{\bullet-}$ in RCs of *Rb. sphaeroides* R26 (not shown). The orientation of the g tensor components of the radical anions of 1,4-benzoquinone and 1,4-naphthoquinone with respect to the molecular frame is such that the g_z axis is perpendicular to the planar π-system and the g_x axis connects the two carbonyl oxygens (Hales, 1975; Burghaus et al., 1993; Füchsle et al., 1993). We expect that MK4 is oriented in the same way as UQ10, since (i) hydrogen bonds fix the positions of the carbonyl oxygens (Allen et al., 1988) and (ii) the C_6-C_{10} ring of the naphthoquinone has a size comparable with that of the two methoxy groups of UQ10. This implies that $D_{PQ} = -0.12$ mT, as for the native RC.

Using this parameter set, the simulation obtained for the X-band ESP spectrum does not resemble the experimental spectrum well (Figure 4B, $J = 0$, compared with Figure 5A). No improvement of the simulation could be obtained while varying structural parameters. Since we are interested in the difference in magnetic interactions of native and MK4-reconstituted RCs, we subsequently focussed on the influence of J_{PQ}. Figure 4 shows that small values of J_{PQ} significantly influence the relative amplitudes of the features in the X-band spectrum of $P^{\bullet+}Q_A^{\bullet-}$. As noted above, we obtain a good correspondence between simulations and the experimental spectra for native and perdeuterated (UQ-containing) RCs at X-band *and* at K-band shown by Füchsle et al. (1993) and Van der Est et al. (1993), using $J_{P\cdot UQ} = -0.9 \pm 0.2$ μT and $\Delta B_{UQ} = 0.60$ mT (see Figure 3). Our X-band spectrum for dark-adapted RCs (shown in Figure 3) is well simulated with $J_{PQ} = -0.4 \pm 0.2$ μT. As mentioned above, small differences in J_{PQ} may be caused by different preparation procedures or biological variability. The X-band spectrum for the MK4-reconstituted RC was simulated using $J_{P\cdot MK} = +0.3 \pm 0.2$ μT and $\Delta B_{MK} = 0.69$ mT (see dashed line in Figure 5). Due to the less anisotropic g tensor of MK4 as compared with that of UQ10, a higher degree of cancellation of the spectral components occurs, such that we could determine unambiguously that orientation I for the g_P tensor is correct. The error margin for the J_{PQ} values is related to a range of ΔB_Q values, such that a decrease of ΔB_Q ($\sim$10 μT) can be compensated by an increase of J_{PQ} ($\sim$0.1 μT). Assuming that MK4 has the same orientation as the native UQ10, the line shape and intensities are reproduced for the mentioned narrow parameter space only (with nonzero J_{PQ}). The change in sign of J_{PQ} ($2J = E_S - E_T$, the energy difference between the radical pair singlet and triplet states) may be attributed to a difference in orbital energies for UQ and MK, related to a difference in the free energy gap ΔG between $P^{\bullet+}Q^{\bullet-}$ and P^* (Gunner & Dutton, 1989; Bixon et al., 1989). Furthermore, it is known from model systems that a small change in bond angles and distances can reverse the sign of J (Knopp & Wieghardt, 1991).

It is interesting to compare the experimental relative magnitudes of J_{PQ} and J_{PI} with those obtained using the well-known empirical distance dependence of J, $J(R) = J(0)e^{-\beta R}$, with $\beta = 17$ nm^{-1} (Moser & Dutton, 1992). We use the value of J_{PI} as an internal reference, since the protein backbone is involved in the electron transfer from P to I, as well as from P to Q, and vice versa. J_{IQ} cannot be used in relation to k_{IQ} for comparison with k_{PQ}, since this is a two-electron integral, related to *double* reduction of Q_A (Okamura et al., 1979b). For $J_{PI} \approx 1$ mT, $R_{PI} = 1.85$ nm, and $R_{PQ} = 2.8$ nm, the empirical relation for $J(R)$ yields $J_{PQ} \approx 1$ nT. The values for J_{PQ} obtained from our simulations are about two orders of magnitude larger. This discrepancy indicates that for short distances the exponential distance dependence of J is strongly modulated by local (superexchange) interactions.

Although we expect that the orientation of the reconstituted quinone will be the same as that of the native acceptor, we searched extensively for other orientational possibilities, rotating the quinone around its g axes. With a fixed $D_{PQ} = -0.12$ mT (and J within the range of -0.5 to $+0.5$ μT), two possible orientations were found for which the spectrum could be simulated accurately: a (counterclockwise) rotation around the g_x axis of $-53°$ and, secondly, a rotation around g_z of $+60°$. Just as for the native orientation, these two orientations were quite sharply defined (to within $\pm 2°$), and intermediate orientations of the g tensor did not yield acceptable simulations. Although a completely different orientation of a substituted quinone is therefore compatible with our analysis of the ESP results, the combination of ESP spectra and considerations concerning hydrogen bonding and molecular size of the quinones leads us to conclude that quinone reconstitution takes place in a well-defined site geometry, set by the protein environment of the Q_A pocket. This finding supports the conclusions on the influence of ΔG_{DA} on electron-transfer rates, obtained from diverse electron-transfer experiments with reconstituted quinones in the RC of *Rb. sphaeroides* R26 (McComb et al., 1990; Schelvis et al., 1992; Moser & Dutton, 1993), which depend directly on the relative orientation of the quinone molecules within the protein matrix.

Comparison with PS I. In principle, simulation of the spin-polarized EPR spectra of the secondary radical pair gives structural information on RCs for which no crystal structure is available, such as the RC of PS I. K-band spectra of $P^{\bullet+}Q^{\bullet-}$ in PS I indicated that the orientation of the phylloquinone is quite different from the orientation of UQ in the Zn^{2+}-substituted RC of *Rb. sphaeroides* R26 (Füchsle et al., 1993). Reconstitution of the bacterial RC with a naphthoquinone allows one to determine whether this difference is intrinsic to the RC protein structures or whether it is a property of the quinone. The X-band spectrum of the spin-polarized secondary radical pair of PS I differs significantly from the spectra of Figure 5 (Snyder et al., 1991). From our simulations we conclude that the reconstituted MK4 has an orientation similar to the UQ in the bacterial RC. Using the g tensors for $P_{700}^{\bullet+}$ (Prisner et al., 1993) and the phylloquinone anion radical (Burghaus et al., 1993) (see Table 1), the experimental ESP spectra of PS I (Snyder et al., 1991) can be simulated when the quinone is rotated $-60°$ around g_z (Füchsle et al., 1993). Thus, the difference

between PS I and the bacterial RC is indeed due to a different orientation of the quinone with respect to the direction of D_{PQ} or to a different value for D_{PQ}, induced by the protein lattice, and not by structural or magnetic differences between phyllo- and ubiquinone in itself.

Spin Polarization of $Q_A^{\bullet-}$. In UQ-containing, Zn^{2+}-substituted RCs, ESP of $Q_A^{\bullet-}$ in prereduced RCs is created by the interaction of the primary radical pair $[P^{\bullet+}I^{\bullet-}]$ with $Q_A^{\bullet-}$ (Gast & Hoff, 1979; Hore, 1990; Hore et al., 1993). Simulations of the emissive EPR spectrum of $Q_A^{\bullet-}$ in perdeuterated, Zn^{2+}-substituted RCs at Q-band (35 GHz) revealed the sign and magnitude of J_{PI} (Hore et al., 1993). These simulations were based on the crystal structure of dark-adapted RCs, and it is legitimate to ask whether freezing in the light would alter the RC structure sufficiently to invalidate the simulations. Our ESP spectra of the spin-polarized $P^{\bullet+}Q_A^{\bullet-}$ radical pair show that the semiquinone anion radical is not displaced with respect to the quinone in the dark-adapted, neutral RC.

The simulations by Hore et al. (1993) were insensitive to the sign and magnitude of the exchange coupling between $I^{\bullet-}$ and the reduced iron–quinone complex, J_{IQ}. This result is confirmed by X-band ESP spectroscopy of prereduced Q_A^- in MK4-reconstituted, Zn^{2+}-substituted RCs of *Rb. sphaeroides* R26. This preparation exhibits a split EPR line when both I and $Q_A{}^{\bullet}Fe^{2+}$ are reduced (Okamura et al., 1979; Tiede et al., 1976; Prince et al., 1977), corresponding to an exchange interaction[3] $|J_{IQ}|$ of 3.0 mT (compared to $|J_{IQ}| \leq$ 0.05 mT for Zn^{2+}-substituted native RCs, and 6.0 mT in RCs of *Rps. viridis*). The light-induced X-band EPR spectrum of prereduced $Q_A^{\bullet-}$ consisted of a clearly emissive ESP line, which was well simulated with the parameters of Hore et al. (1993) (data not shown). This experiment inspires confidence in the determination of J_{PI} by Hore et al. (1993).

The interaction of the primary radical pair ($P^{\bullet+}I^{\bullet-}$) with a third spin ($Q_A^{\bullet-}$), however, does not only create electron spin polarization on $Q_A^{\bullet-}$ but is also expected to affect the spin evolution of $P^{\bullet+}I^{\bullet-}$ (Hore et al., 1988). We, therefore, studied the electron spin polarization of the triplet state of the primary donor, ^3P, and its temperature dependence for RCs of *Rb. sphaeroides* R26 under different conditions.

The Polarization Pattern of ^3P. In prereduced RCs, ^3P is formed in high magnetic fields by exclusive mixing of the $m_s = 0$ triplet state sublevel of the primary radical pair ($P^{\bullet+}I^{\bullet-}$) with its singlet state, the so-called $S-T_0$ mixing process. The EPR signal of ^3P shows a remarkable temperature dependence in photosynthetic purple bacteria that contain menaquinone as Q_A (Van Wijk et al., 1987, 1988; Van Wijk & Schaafsma, 1988). A pronounced anisotropy in the ESP is observed: at the canonical *X* direction of ^3P the ESP is apparently temperature *in*dependent, as distinct from the canonical *Y* and *Z* directions. We have demonstrated that exchange-mediated anisotropic spin–lattice relaxation in the primary radical pair triplet state is the primary cause of this phenomenon in MK-containing bacteria (Van den Brink et al., 1994).

In RCs of *Rb. sphaeroides* R26, we use the ratio of the amplitudes of the canonical *Y* and *X* directions under continuous illumination as a measure of the influence of the quinone at the Q_A site on the spin dynamics of the primary radical pair and consequently on the relative populating

[3] We use the convention that the splitting between the two $I^{\bullet-}$ lines is 2*J*.

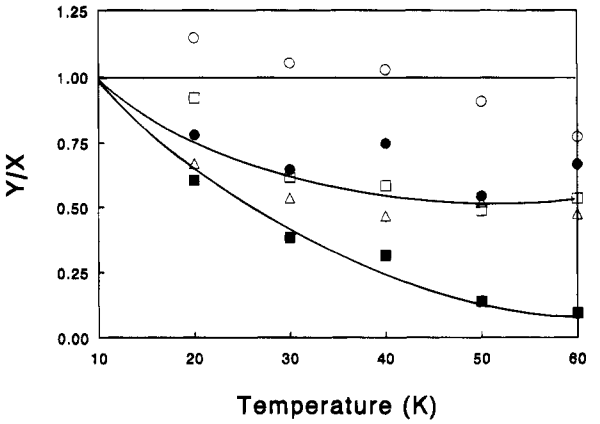

FIGURE 6: Temperature dependence of the ESP EPR signals from ^3P in native (△), Zn^{2+}-substituted (●), quinone-depleted (○), MK4-reconstituted, Fe^{2+}-containing (■), and MK4-reconstituted, Zn^{2+}-substituted (□) RCs of *Rb. sphaeroides* R26. Under light-modulation conditions, the canonical *Y* direction is sensitive, and the canonical *X* direction is insensitive to an increase of temperature, except for quinone-depleted RCs. The ratio of amplitudes of the canonical *Y* and *X* direction, normalized at 10 K, is used as an indicator of the interaction of the primary radical pair with a third spin on Q_A. All spectra were obtained using 370-Hz light modulation. The lines are drawn as a guide to the eye.

probabilities of the three sublevels of ^3P. Figure 6 shows the temperature dependence of the *Y/X* ratio for light-modulated EPR spectra of ^3P in RCs of *Rb. sphaeroides* R26 under different conditions. The light-modulation frequency is low in comparison with the decay rates of ^3P, so that steady-state conditions obtain.

In the absence of the quinone, the observed *Y/X* ratio for ^3P under steady-state conditions is not temperature dependent, indicating that the primary radical pair does not interact with any other radical. In this "pure" radical pair, the triplet state is created in its T_0 state exclusively at all temperatures, resulting in the unique AEEAAE polarization pattern [see Hoff (1984) and references cited therein]. This result shows that ^3P oriented at the canonical *X* and *Y* directions has similar *steady*-state populations at all temperatures in quinone-depleted RCs. Since the triplet-sublevel decay rates at high magnetic fields are comparable for ^3P oriented at the canonical *X* and *Y* directions, it follows that spin–lattice relaxation at the canonical *X* and *Y* directions of ^3P is largely independent of orientation in the *X*–*Y* plane in quinone-depleted RCs. For quinone-containing RCs, therefore, observed differences in the *Y/X* ratio reflect a difference of the *initial* population of the sublevels of the canonical *Y* direction of ^3P relative to that of the canonical *X* direction.

In the native, Q_A-containing RC, only a slight temperature dependence is observed, related to the relatively small J_{IQ} for ubiquinone (~0.05 mT (Okamura et al., 1979a). Therefore, the relaxation of the primary radical pair triplet state is not enhanced to a degree comparable with k_T, the rate of the primary radical pair's decay to ^3P, which is approximately 4×10^8 s^{-1} (Goldstein & Boxer, 1989a). In the case of *Rps. viridis*, which contains MK9 and where $J_{IQ} \approx 6$ mT, enhanced relaxation, mediated by the 100-fold larger J_{IQ}, causes the pronounced temperature dependence of the *Y/X* ratio of ^3P (Van den Brink et al., 1994). Concordantly, the temperature dependence of the *Y/X* ratio of ^3P in MK4-reconstituted, Fe^{2+}-containing RCs of *Rb. sphaeroides* R26 is much more pronounced than that in the native RC (Figure 6) and comparable to results reported for MK8-reconstituted RCs (Van Wijk et al., 1988), indicating a value for J_{IQ} that

is of the same order of magnitude as that in *Rps. viridis*. This was confirmed by the observation of the characteristic AB-like spectrum for $I^{\bullet-}$ in MK4-reconstituted RCs ($|J_{IQ}| = 3.0$ mT, data not shown).

Temperature Dependence of ^3P in Zn^{2+}-Substituted RCs. Upon removal of the Fe^{2+} ion, the $g = 1.8$ EPR signal, attributed to the $Fe^{2+}Q_A^{\bullet-}$ complex (Butler et al., 1984), is absent, and a $g = 2.0048$ EPR line is observed for $Q_A^{\bullet-}$. This slowly relaxing semiquinone anion radical in Fe^{2+}-depleted RCs [$T_1 \approx 5$ s at 4 K (Gast et al., 1982)] cannot enhance the relaxation in the primary radical pair to a rate comparable with k_T. Nevertheless, in Zn^{2+}-substituted (both UQ- *and* MK-containing) RCs, a temperature dependence of ^3P is observed, which is comparable to that in native RCs. On the basis of the temperature *in*dependence of the *Y*/*X* ratio in quinone-depleted RCs, we can exclude relaxation effects of ^3P, so that the temperature dependence in Zn^{2+}-substituted RCs must be related to the creation of $T_\pm$ population within the primary radical pair.

The temperature-dependent population of the $T_\pm$ sublevels has a different physical origin in Fe^{2+}-containing and in Zn^{2+}-substituted RCs, namely, an incoherent relaxation process in the primary radical pair triplet state in the former (Van den Brink et al., 1994) and coherent singlet−triplet mixing in the three-spin radical complex $[P^{\bullet+}I^{\bullet-}Q_A^{\bullet-}]$ in the latter case (Hore et al., 1988). In Fe^{2+}-containing RCs, the $g = 1.8$ $Fe^{2+}Q_A^{\bullet-}$ spin system enhances (fast) spin−lattice relaxation in the primary radical pair triplet state $^3[P^{\bullet+}I^{\bullet-}]$ via J_{IQ}, thus populating its $T_\pm$ sublevels. Recombination then populates, in addition to T_0, the $T_\pm$ sublevels ($m_s = \pm 1$) of ^3P, because of conservation of angular momentum. In Zn^{2+}-substituted RCs, on the contrary, the (slowly relaxing) $g = 2.0$ electron spin of the semiquinone anion effectively couples with the primary radical-pair states, forming the three-spin radical complex $[P^{\bullet+}I^{\bullet-}Q_A^{\bullet-}]$. In this complex, a coherent mixing process populates the $T_\pm$ sublevels of ^3P, concomitantly producing spin polarization of $Q_A^{\bullet-}$ (Gast & Hoff, 1979; Hore et al., 1988, 1993). The relative populations of the triplet sublevels of the primary radical pair in Zn^{2+}-substituted RCs are related to the interaction between $I^{\bullet-}$ and $Q_A^{\bullet-}$ and to the relaxation rate of the quinone spin [see Figure 6 in Hore et al. (1988)]. The fact that we observe anisotropy for the temperature dependence of the ESP of ^3P for Zn^{2+}-substituted RCs again evidences that the magnetic interaction between $I^{\bullet-}$ and $Q_A^{\bullet-}$ is remarkably anisotropic (Hore et al., 1993). This implies that the g axis of $Q_A^{\bullet-}$, for which this molecule has the longest T_1 and/or the smallest interaction with $I^{\bullet-}$, coincides with the canonical X direction of ^3P. From the crystal structure, it is seen that the g_z axis of UQ10, which is expected to be the direction with the longest T_1, indeed coincides with the canonical X direction of ^3P: the angle between $X(^3P)$ and $g_z(Q_A^{\bullet-})$ is 3.6°. Thus, using Zn^{2+}-substituted, MK4-reconstituted RCs of *Rb. sphaeroides* R26, we obtained additional evidence for the model of Hore and co-workers (Hore et al., 1988, 1993) for concomitant development of electron spin polarization in $Q_A^{\bullet-}$ and ^3P during the lifetime of $[P^{\bullet+}I^{\bullet-}Q_A^{\bullet-}]$ in prereduced, Zn^{2+}-substituted RCs of *Rb. sphaeroides* R26.

CONCLUSIONS

We have studied the structure−function relationship of the bacterial photosynthetic RC, and especially the position and orientations of the first quinone molecule (Q_A) involved in charge separation and stabilization, using time-resolved EPR. The spin-polarized EPR spectrum of the secondary radical pair, $P^{\bullet+}Q_A^{\bullet-}$, whose shape critically depends on the RC-structure, is essentially the same for RCs of *Rb. sphaeroides* R26 frozen in the dark and under continuous illumination. Simulations showed that no major reorientation of the Q_A acceptor for RCs frozen in the charge-separated state can occur, and we conclude that the differences in $P^{\bullet+}Q_A^{\bullet-}$ recombination times observed earlier (Kleinfeld et al., 1984), and confirmed in this work, are most likely related to (small) light-induced conformational changes in the protein matrix, affecting the electron affinity of $Q_A^{\bullet-}$ by changing the orientation of its methoxy substituents. The time-resolved EPR line shapes are shown to be very sensitive to the nature of the quinone at Q_A. A major difference reported previously (Van Wijk & Schaafsma, 1988; Van den Brink, 1994) is the temperature dependence of the ESP pattern of ^3P, which is related to the magnitude of the exchange interaction J_{IQ}, obtained from the AB-like spectrum of the reduced intermediary acceptor $I^{\bullet-}$ (Prince et al., 1977). We show that the larger value of J_{IQ} has no marked influence on the spin polarization of the prereduced quinone in Zn^{2+}-reconstituted RCs. The difference observed for the ESP of the secondary radical pair is shown to be mainly due to the difference in g values of UQ and MK. On the basis of spectral simulations, we conclude that the orientation of the reconstituted MK4 is identical with that of UQ10 in the native RC. From our simulations of the X-band ESP spectra, we conclude that J_{PQ} has a small but finite value, viz. $J_{P\text{-}UQ} = (-0.8 \pm 0.2)$ μT, and $J_{P\text{-}MK} = (+0.3 \pm 0.2)$ μT. Since the structure of the bacterial RC is not altered when UQ is replaced by MK, differences observed for the ESP patterns of the secondary radical pair in purple bacteria and in PS I are most likely due to an intrinsic difference in the structure of the binding pocket of the quinone molecule.

ADDED IN PROOF

A recent W-band (95 GHz) EPS study of Zn^{2+}-substituted RCs of *Rb. sphaeroides* R26 (Prisner et al., 1994) indicates that orientation II of the g tensor of P^+ gives a better description of the spin-polarized spectrum of $P^+Q_A^-$ than does orientation I at this frequency. However, all attempts to simulate our X-band ESP spectra using orientation II, both for native and MK4-reconstituted RCs, give quite unsatisfactory results, unless large, and in our opinion unrealistic (>15°) rotations of Q_A are introduced.

ACKNOWLEDGMENT

We thank Dr. G. Zwanenburg for helpful discussions, Mr. A. H. M. de Wit for growing the bacteria, and Ms. S. J. Jansen for help with preparing the RCs. We also thank Dr. A. van der Est (Free University, Berlin) for sending us the digitized X-band ESP spectrum of protonated RCs. Menaquinone-4 was a gift from F. Hoffmann-La Roche & Co., Switzerland.

REFERENCES

Allen, J. P., Feher, G., Yeates, T. O., Komiya, H., & Rees, D. C. (1988) *Proc. Natl. Acad. Sci. U.S.A. 85*, 8487−8491.

Bencini, A., & Gatteschi, D. (1990) *EPR of Exchange Coupled Systems*, Springer-Verlag, Berlin.

Beratan, D. N., & Hopfield, J. J. (1984) *J. Am. Chem. Soc. 106*, 1584−1594.

Bixon, M., Jortner, J., Michel-Beyerle, M. E., & Ogrodnik, A. (1989) *Biochim. Biophys. Acta 977*, 273−286.
Bixon, M., Jortner, J., & Michel-Beyerle, M. E. (1991) *Biochim. Biophys. Acta 1056*, 301−315.
Brzezinski, P., Okamura, M. Y., & Feher, G. (1992) in *The Photosynthetic Bacterial Reaction Center II* (Breton, J., & Verméglio, A., Eds.) pp 321−330, Plenum Press, New York.
Burghaus, O., Plato, M., Rohrer, M., Möbius, K., McMilland, F., & Lubitz, W. (1993) *J. Phys. Chem. 97*, 7639−7647.
Butler, W. F., Calvo, R., Fredkin, D. R., Isaacson, R. A., Okamura, M. Y., & Feher, G. (1984) *Biophys. J. 45*, 947−973.
Collins, A. J., & Jones, D. (1981) *Microbiol. Rev. 45*, 316−354.
Debus, R. J., Feher, G., & Okamura, M. Y. (1986) *Biochemistry 25*, 2276−2287.
Feher, G., & Okamura, M. Y. (1978) in *The Photosynthetic Bacteria* (Clayton, R. K., & Sistrom, W. R., Eds.) pp 349−386, Plenum Press, New York.
Füchsle, G., Bittl, R., Van der Est, A., Lubitz, W., & Stehlik, D. (1993) *Biochim. Biophys. Acta 1142*, 23−35.
Gast, P., & Hoff, A. J. (1979) *Biochim. Biophys. Acta 548*, 520−535.
Gast, P., Mushlin, R. A., & Hoff, A. J. (1982) *J. Phys. Chem. 86*, 2886−2891.
Gast, P., De Groot, A., & Hoff, A. J. (1983) *Biochim. Biophys. Acta 723*, 52−58.
Gast, P., Hemelrijk, P., & Hoff, A. J. (1994) *FEBS Lett. 337*, 39−42.
Goldstein, R. A., & Boxer, S. G. (1989a) *Biochim. Biophys. Acta 977*, 70−77.
Goldstein, R. A., & Boxer, S. G. (1989b) *Biochim. Biophys. Acta 977*, 78−86.
Gunner, M. R., & Dutton, P. L. (1989) *J. Am. Chem. Soc. 111*, 3400−3412.
Hales, B. J. (1975) *J. Am. Chem. Soc. 97*, 5993−5997.
Hiraishi, A., & Hoshino, Y. (1984) *J. Gen. Appl. Microbiol. 30*, 435−448.
Hoff, A. J. (1984) *Q. Rev. Biophys. 17*, 153−182.
Hoff, A. J., Gast, P., & Romijn, J. C. (1977) *FEBS Lett. 73*, 185−190.
Hore, P. J. (1990) in *Advanced EPR, Applications in Biology and Biochemistry* (Hoff, A. J., Ed.) pp 405−438, Elsevier Publishers, Amsterdam.
Hore, P. J., Hunter, D. A., McKie, C. D., & Hoff, A. J. (1987) *Chem. Phys. Lett. 137*, 495−500.
Hore, P. J., Hunter, D. A., Van Wijk, F. G. H., Schaafsma, T. J., & Hoff, A. J. (1988) *Biochim. Biophys. Acta 936*, 249−258.
Hore, P. J., Riley, D. J., Semlyen, J. J., Zwanenburg, G., & Hoff, A. J. (1993) *Biochim. Biophys. Acta 1141*, 221−230.
Jortner, J. (1976) *J. Chem. Phys. 64*, 4860−4867.
Kleinfeld, D., Okamura, M. Y., & Feher, G. (1984) *Biochemistry 23*, 5780−5786.
Klette, R., Törring, J. T., Plato, M., Möbius, K., Bönigk, B., & Lubitz, W. (1993) *J. Phys. Chem. 97*, 2015−2020.
Komiya, H., Yeates, T. O., Rees, D. C., Allen, J. P., & Feher, G. (1988) *Proc. Natl. Acad. Sci. U.S.A. 85*, 9012−9016.
Knopp, P., & Wieghardt, K. (1991) *Inorg. Chem. 30*, 4061−4066.
Lersch, W., Lendzian, F., Lang, E., Feick, R., Möbius, K., & Michel-Beyerle, M. E. (1989) *J. Magn. Reson. 82*, 143−149.
Liu, B.-L., Yang, L.-H., & Hoff, A. J. (1991a) *Photosynth. Res. 28*, 51−58.
Liu, B.-L., Van Kan, P. J. M., & Hoff, A. J. (1991b) *FEBS Lett. 289*, 23−28.
Marcus, R. A. (1956) *J. Chem. Phys. 24*, 966−978, 979−989.
Marcus, R. A., & Sutin, N. (1985) *Biochim. Biophys. Acta 811*, 265−322.
McComb, J. C., Stein, R. R., & Wraight, C. A. (1990) *Biochim. Biophys. Acta 1015*, 156−171.
Michel-Beyerle, M. E., Plato, M., Deisenhofer, J., Michel, H., Bixon, M., & Jortner, J. (1988) *Biochim. Biophys. Acta 932*, 52−70.
Moser, C. C., & P. L. Dutton (1992) *Biochim. Biophys. Acta 1101*, 171−176.
Muus, L. T., Atkins, P. W., McLauchlan, K. A., & Pedersen, J. B., Eds. (1977) *Chemically Induced Magnetic Polarization*, Reidel, Dordrecht, The Netherlands.
Norris, J. R., Lin, C. P., & Budil, D. (1987) *J. Chem. Soc., Faraday Trans. I 83*, 13−27.
Okamura, M. Y., Isaacson, R. A., & Feher, G. (1979a) *Biochim. Biophys. Acta 546*, 394−417.
Okamura, M. Y., Fredkin, D. R., Isaacson, R. A., & Feher, G. (1979b) in *Tunneling in Biological Systems* (Chance, B., DeVault, D. C., Frauenfelder, H., Marcus, R., Schrieffer, J. R., & Sutin, N., Eds.) pp 729−743, Academic Press, New York.
Parot, P., Thiery, J., & Verméglio, A. (1987) *Biochim. Biophys. Acta 893*, 534−543.
Parson, W. W., & Warshel, A. (1993) in *The Photosynthetic Reaction Center* (Deisenhofer, J., & Norris, J. R., Eds.) Vol. II, pp 23−47, Academic Press, New York.
Plato, M., Möbius, K., Michel-Beyerle, M. E., Bixon, M., & Jortner, J. (1988) *J. Am. Chem. Soc. 110*, 7279−7285.
Prince, R. C., Tiede, D. M., Thornber, J. P., & Dutton, P. L. (1977) *Biochim. Biophys. Acta 462*, 467−490.
Prisner, T. F., McDermott, A. E., Un, S., Norris, J. R., Thurnauer, M. C., & Griffin, R. G. (1993) *Proc. Natl. Acad. Sci. U.S.A. 90*, 9485−9488.
Prisner, T. F., van der Est, A., Bittl, R., Lubitz, W., Stehlik, D., & Möbius, K. (1994) *Chem. Phys.* (in press).
Proskuryakov, I. I., Shkuropatov, A. Y., Voznyak, V. M., & Shuvalov, V. A. (1988) *Biofizika 33*, 877−879.
Robinson, H. H., & Kahn, S. D. (1990) *J. Am. Chem. Soc. 112*, 4728−4731.
Schelvis, J. P. M., Liu, B.-L., Aartsma, T. J., & Hoff, A. J. (1992) *Biochim. Biophys. Acta 1102*, 229−236.
Siddarth, P., & Marcus, R. A. (1993) *J. Phys. Chem. 97*, 2400−2405.
Shopes, R. J., & Wraight, C. A. (1985) *Biochim. Biophys. Acta 806*, 348−356.
Snyder, S. W., & Thurnauer, M. C. (1993) in *The Photosynthetic Reaction Center* (Deisenhofer, J., & Norris, J. R., Eds.) Vol. II, pp 285−329, Academic Press, New York.
Snyder, S. W., Rustandi, R. R., Biggins, J., Norris, J. R., & Thurnauer, M. C. (1991) *Proc. Natl. Acad. Sci. U.S.A. 88*, 9895−9896.
Stehlik, D., Bock, C. H., & Petersen, J. (1989) *J. Phys. Chem. 93*, 1612−1619.
Tiede, D. M., Prince, R. C., & Dutton, P. L. (1976), *Biochim. Biophys. Acta 449*, 447−467.
Tiede, D. M., & Dutton, P. L. (1981) *Biochim. Biophys. Acta 637*, 278−290.
Van den Brink, J. S., Gast, P., Manikowski, H., & Hoff, A. J. (1994) *Biochim. Biophys. Acta* 1185, 177−187.
Van der Est, A., Bittl, R., Abresch, E. C., Lubitz, W., & Stehlik, D. (1993) *Chem. Phys. Lett. 212*, 561−568.
Van der Vos, R. (1994) Dissertation, Leiden University.
Van Wijk, F. G. H., & Schaafsma, T. J. (1988) *Biochim. Biophys. Acta 936*, 236−248.
Van Wijk, F. G. H., Beijer, C. B., Gast, P., & Schaafsma, T. J. (1987) *Photobiochem. Photobiol. 46*, 1015−1019.
Van Wijk, F. G. H., Gast, P., & Schaafsma, T. J. (1988) *Photobiochem. Photobiophys. 11*, 95−100.
Woodbury, N., & Parson, W. W. (1984) *Biochim. Biophys. Acta 747*, 345−361.